

# Optimal Controllers for DFIG based Wind Farm connected to Grid using Evolutionary Techniques

M. Abd-Elkareem<sup>1</sup>, E.Abd-Elalim<sup>2</sup>, M.A. Ebrahim<sup>3</sup>

<sup>1</sup>Demonstrator, <sup>2</sup>Professor, <sup>3</sup>Doctor

<sup>1</sup>High Institute of Engineering, El Shorouk Academy, Cairo, Egypt

<sup>2</sup>Faculty of Engineering, Ain Shams University, Cairo, Egypt

<sup>3</sup>Faculty of Engineering at Shoubra, Benha University, Cairo, Egypt

**Abstract:** Optimal control of wind systems has become a critical issue for the development of renewable energy systems and their integration into grid to provide reliable, secure, and efficient electricity. Among many enabling technologies, a new method using particle swarm optimization (PSO) is proposed for optimizing the parameters of different types of controllers for a doubly fed induction generator (DFIG) based wind farm connected to grid. New objective function is illustrated with the PSO-based optimization algorithm to optimize the controllers' parameters. The implementation of the algorithm is described in detail and compared with the Genetic Algorithm (GA). In this paper, the generic dynamic model of WT with DFIG and its associated controllers (pitch controller, rotor side converter controller, and grid side converter controller) are presented. Initially PI controllers are used then compared to PID controllers using PSO. With the PSO-PID optimized controllers, the system stability is improved under large and small disturbances as well the dynamic performance of the WT with DFIG can be improved. Simulations using MATLAB/SIMULIK are performed to illustrate the controllers' performance.

**Keywords:** Optimal control, Particle Swarm Optimization, Doubly Fed Induction Generator, Genetic Algorithm.

## I. INTRODUCTION

Nowadays wind generationsystems penetration into electric networks is increasing worldwide encouraged by national and international policies aiming to increase the share of renewable energy sources and highly efficient micro-combined heat and power units in order to reduce greenhouse gas emissions and alleviate global warming. Next to environmental advantages, wind generation systems contribute in the application of competitive energy policies, diversification of energy resources, reduction of on-peak operating cost, deferral of network upgrades, lower losses and lower transmission and distribution costs, and potential increase of service quality to the end-customer. DFIG is widely used in the wind power system for its advantages over other wind turbine generators, such as squirrel-cage induction generator and permanent magnet synchronous generator [1]. The characteristics of DFIG are high efficiency, flexible control and low investment. The stator of DFIG is directly connected to the power grid while the rotor is connected to the power grid through a back-to-back converter, which only takes about 20%–30% of the DFIG rated capacity for the reason that the converter only supplies the exciting current of the DFIG. The back-to-back converter consists of three parts: rotor side converter (RSC), grid side converter (GSC), and dc link capacitor. The controllers of the converter have significant effect on the stability of grid-connected DFIG [2].

In previous research, the optimal control of WT with DFIG had been studied by many researchers [3-5]. One of the key challenges for DFIG based wind farm optimization is the involvement of a large number of parameters need to be optimized to ensure a good interaction of the wind power with the power grid at the common coupling point (CCP). For instance, in [6], the authors presented an approach to use PSO to optimize all the controllers' parameters in a DFIG. This method can improve the performance of the DFIG in the power grid, however, when the number of the DFIG in a wind farm increases, the number of the control parameters will increase significantly. Therefore, advanced

coordinated control approaches such as adaptive dynamic programming (ADP) based methods have showed great success and promising for such a challenging problem [7-9].

In this paper, new procedure using PSO algorithm is used to find the optimal parameters for the various controllers (pitch angle controller, rotor-side converter controller and grid side converter controller) of DFIG based wind farm connected to grid. Different types of controllers PI, and PID can be used, tuned and compared. New time-domain fitness function is defined to measure the performance of the controllers. Simulation results show that the proposed design approach is efficient to find the optimal parameters of the controllers and therefore improves the transient performance of the wind turbine generator system (WTGS) over a wide range of operating conditions. System modeling with controllers is carried out using MATLAB/SIMULINK to verify the effectiveness of proposed method and various simulation results are discussed.

## II. POWER SYSTEM MODEL

The studied model here as shown in Fig. 1 consists of a wind farm of 9 MW capacity consisting of six 1.5 MW wind turbines connected to a 25 kV distribution system exports power to a 120 kV grid through a 30 km, 25 kV feeder. Wind turbines using a DFIG consist of a wound rotor induction generator and an AC/DC/AC IGBT-based PWM converter. The stator winding is connected directly to the 60 Hz grid while the rotor is fed at variable frequency through the AC/DC/AC converter. The DFIG technology allows extracting maximum energy from the wind for low wind speeds by optimizing the turbine speed, while minimizing mechanical stresses on the turbine during gusts of wind. The wind speed is maintained constant at 15 m/s. The control system uses a torque controller in order to maintain the speed at 1.2 pu. The reactive power produced by the wind turbine is regulated at 0 Mvar. The detailed model of the DFIG wind turbine system is introduced in this research [10].

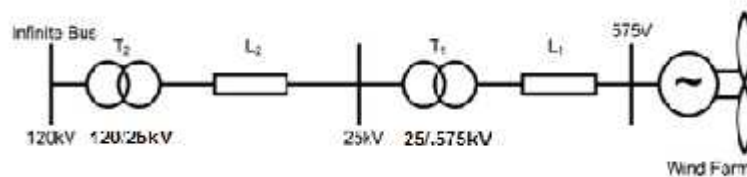


Fig. 1 Single-line diagram of the power system under study.

## III. DFIG WIND TURBINE SYSTEM MODEL

The DFIG wind turbine model is illustrated in Fig. 2. In this system, the wind turbine is connected to the DFIG through a drive train system, which consists of a low and a high speed shaft with a gearbox in between. The DFIG system is an induction type generator in which the stator windings are directly connected to the three-phase grid and the rotor windings are fed through three-phase back-to-back IGBT based PWM converters. The back-to-back PWM converter consist of three parts: a rotor side converter (RSC), a grid side converter (GSC) and a dc link capacitor placed between the two converters. The controllers consist of three parts: rotor side controller, grid side controller and wind turbine controller. The functions of these controllers are to produce smooth electrical power with constant voltage and frequency to the power grid whenever the wind system is working at sub-synchronous speed or super-synchronous speed, depending on the velocity of the wind. Vector control strategy is employed for both the RSC and GSC to achieve decoupled control of active and reactive power.

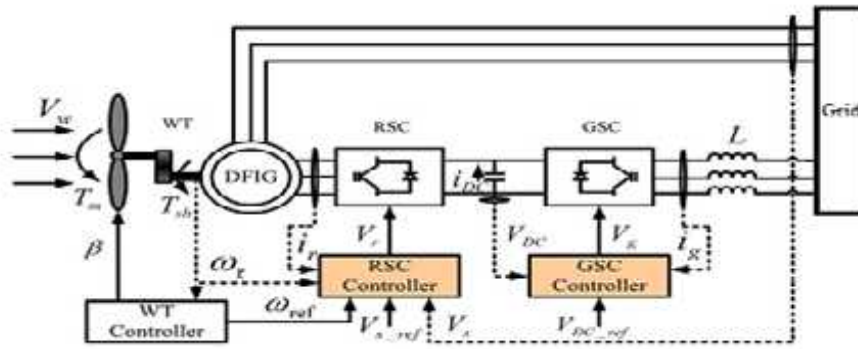


Fig. 2 Schematic diagram of DFIG wind turbine system.

### A. Dynamic Model of DFIG

In order to investigate the actual behavior of the DFIG, dynamic equation needs to be considered for more realistic observation. From the point of view of the control of the machine, the dq representation of an induction machine leads to control flexibility. The dynamic behavior of the DFIG in synchronous reference frame can be represented by the Park equations provided all the rotor quantities are referred to the stator side. The stator and rotor voltages are expressed as follows:

$$v_d = R_s i_d + \frac{d\phi_d}{dt} - \omega_s \phi_q \quad (1)$$

$$v_q = R_s i_q + \frac{d\phi_q}{dt} + \omega_s \phi_d \quad (2)$$

$$v_d = R_r i_d + \frac{d\phi_d}{dt} - (\omega_s - \omega_r) \phi_q \quad (3)$$

$$v_q = R_r i_q + \frac{d\phi_q}{dt} + (\omega_s - \omega_r) \phi_d \quad (4)$$

The flux linkage equations of the stator and rotor can be related to their currents and are expressed as follows:

$$\phi_d = L_s i_d + L_m i_d \quad (5)$$

$$\phi_q = L_s i_q + L_m i_q \quad (6)$$

$$\phi_d = L_r i_d + L_m i_d \quad (7)$$

$$\phi_q = L_r i_q + L_m i_q \quad (8)$$

where,  $L_{ss} = L_s + L_m$  and  $L_{rr} = L_r + L_m$

The electromagnetic torque developed by the DFIG is related to the torque supplied by the turbine and can be expressed as:

$$T_e = 1.5p(\phi_d i_q - \phi_q i_d) = 2H \frac{d\omega_m}{dt} + B\omega_m + T_m \quad (9)$$

where,  $T_m$  is positive for motoring operation and negative for generator operation. Equations(1) to (9) are the set of differential equations which represent a fourth order model for describing the dynamic behavior of DFIG.

### B. Wind Turbine Dynamic Model

The wind turbine model provides a simplified representation of a very complex electromechanical system. In simple terms, the function of the wind turbine is to extract as much power from the available wind as possible without exceeding the rating of the equipment. The wind turbine model represents all of the relevant controls and mechanical dynamics of the wind turbine. A wind turbine dynamic model usually contains the following elements representing its basic functional components as shown in Fig.

3, the wind turbine aero-dynamic model, the wind turbine drive train model, the model of the DFIG induction generator fitted with a back-to-back converter in the rotor circuit, and electric grid model and the wind turbine control system model.

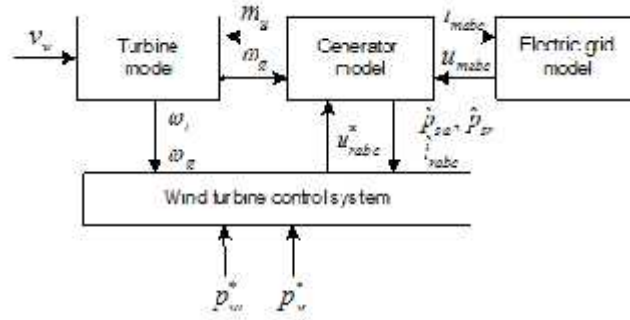


Fig. 3 Block diagram of the dynamic model of a wind turbine connected to grid.

#### IV. CONTROL MODELS

##### A. Pitch Angle Control Model

Pitch controller is used to control the blade pitch angle in order to limit the electric output power to the nominal mechanical power. The pitch angle is kept constant at zero degree when the measured electric output power is under its nominal value. When it increases above its nominal value the controller increases the pitch angle to bring back the measured power to its nominal value. The control system model is illustrated in Fig. 4.

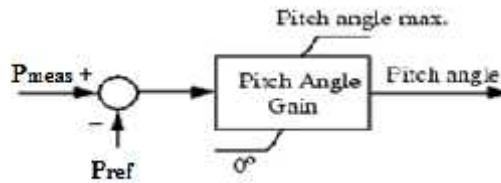


Fig. 4 Pitch angle control model.

##### B. Rotor Side Converter Control Model

Rotor side converter control model is shown in Fig. 5. For the rotor side controller the d-axis of the rotating reference frame used for d-q transformation is aligned with air-gap flux. The actual electrical output power, measured at the grid terminals of the wind turbine, is added to the total power losses (mechanical and electrical) and is compared with the reference power. Controller is used to reduce the power error to zero. The output of this regulator is the reference rotor current  $I_{qr\_ref}$  that must be injected in the rotor by RSC. This is the current component that produces the electromagnetic torque  $T_{em}$ . The actual  $I_{qr}$  component is compared to  $I_{qr\_ref}$  and the error is reduced to zero by a current regulator. The output of this current controller is the voltage  $V_{qr}$  generated by RSC. The current regulator is assisted by feed forward terms which predict  $V_{qr}$ . The voltage at grid terminals is controlled by the reactive power generated or absorbed by the RSC. The reactive power is exchanged between RSC and the grid, through the generator. In the exchange process the generator absorbs reactive power to supply its mutual and leakage inductances. The excess of reactive power is sent to the grid or to RSC. The output of the voltage regulator or the var regulator is the reference d-axis current  $I_{dr\_ref}$  that must be injected in the rotor by RSC.

The same current regulator as for the power control is used to regulate the actual  $I_{dr}$  component of positive-sequence current to its reference value. The output of this regulator is the d-axis voltage  $V_{dr}$  generated by RSC. The current regulator is assisted by feed forward terms which predict  $V_{dr}$ .  $V_{dr}$  and  $V_{qr}$  are respectively the d-axis and q-axis of the voltage  $V_r$ .

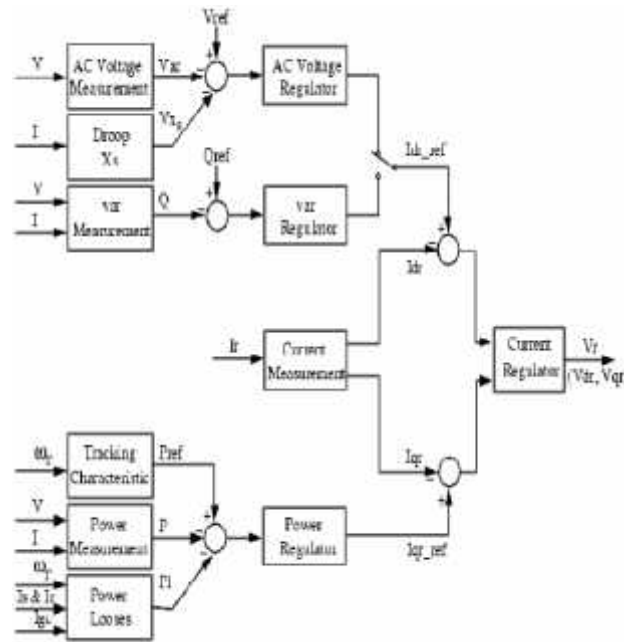


Fig. 5 Rotor side converter control model.

### C. Grid Side Converter Control Model

The grid side converter is used to regulate the voltage of the DC link between the two converters. As shown in Fig. 7. the GSC contains an outer loop control that controls the DC-link voltage, attempting to control it to nominal value and an inner control loop controls the GSC current. Commonly the GSC acts to set  $Q_{ge} = 0$  and maximize active power output. As the GSC is connected directly to the grid, it must output power at a fixed frequency corresponding to the grid frequency. The GSC voltage equations are obtained in (10), which gives:

$$\begin{aligned}
 v_{as} &= R i_{as} + L \frac{di_{as}}{dt} + e_a \\
 v_{bs} &= R i_{bs} + L \frac{di_{bs}}{dt} + e_b \\
 v_{cs} &= R i_{cs} + L \frac{di_{cs}}{dt} + e_c
 \end{aligned}
 \tag{10}$$

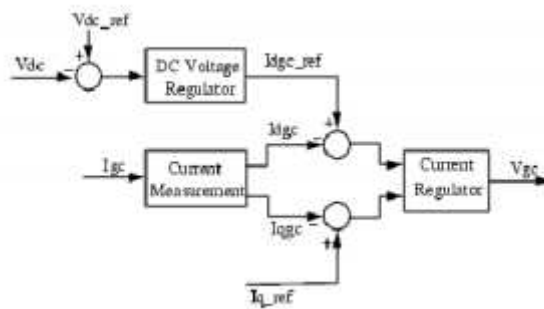


Fig. 6 Grid side converter control model.

## V. OPTIMIZATION OF CONTROLLERS USING PSO

In this section the parameters of the proposed controllers (pitch angle controller, rotor side converter current regulator, and grid side converter current regulator) are optimally tuned using PSO. In optimization methods, the first step is to define a performance index for optimal search. In this study the performance index is considered as (11). It can be Integral of the Time multiplied Absolute Error (ITAE). It is clear to understand that the controller with lower performance index is better than the other controllers. To compute the optimum parameter values, we will observe the steady-state

operation of the DFIG and its dynamic response. It should be noted that PSO algorithm is run several times and then optimal set of parameters is selected.

The overall design procedure is shown in the flowchart of Fig. 7. The efforts and optimum values of parameters obtained using PSO-PI and PSO-PID are compared to GA-PI and summarized in Table I and TableII. In addition, the time response for P, Q, and  $V_{dc}$  is shown in Fig. 8 to Fig. 10.

$$ITAE = \int_0^t |e(t)| .dt \quad (10)$$

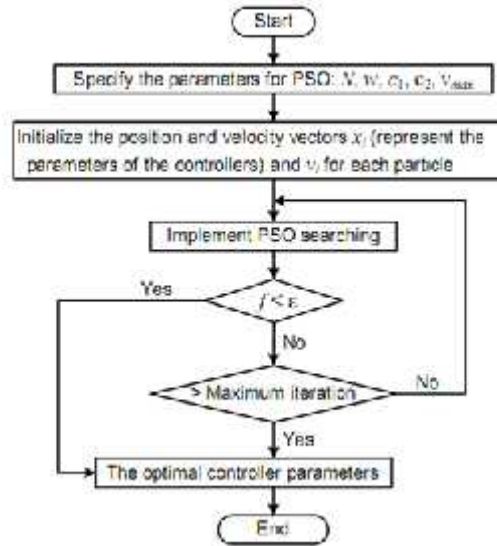


Fig. 7 Optimal controller parameters design procedure flow chart.

TABLE I  
 THE EFFORTS OF THE PSO AND GA WITH PI & PID CONTROLLERS IN SIMULATION

Response	Method	ITAE
rising time (sec)	PI	0.0033
	PI- GA	0.0033
	PI-PSO	0.0031
	PID-PSO	0.0032
over shoot (percent)	PI	32.7935
	PI- GA	49.3872
	PI-PSO	39.5403
	PID-PSO	33.5435
settling time (sec)	PI	0.0698
	PI- GA	0.1898
	PI-PSO	0.1724
	PID-PSO	0.0758
steady state error	PI	1.68e-6
	PI- GA	7.74e-8
	PI-PSO	1.67e-6
	PID-PSO	2.50e-7

TABLE II  
 OPTIMAL PARAMETERS OBTAINED FOR DIFFERENT CONTROLLERS

Parameter	Method	Pitch controller	RSC current regulator	GSC current regulator
$K_p$	PI	3	0.6	0.83
	PI- GA	1.24	0.213	0.654
	PI-PSO	2.66	0.3139	0.551
	PID-PSO	3.06	0.5259	0.851
$K_i$	PI	30	8	5
	PI- GA	19.55	6.012	3.2211
	PI-PSO	25.1389	6.3475	5.2175
	PID-PSO	28.1389	8.2049	6.6175
$K_d$	PI	--	--	--
	PI- GA	--	--	--
	PI-PSO	--	--	--
	PID-PSO	0.032	0.0874	0.0776

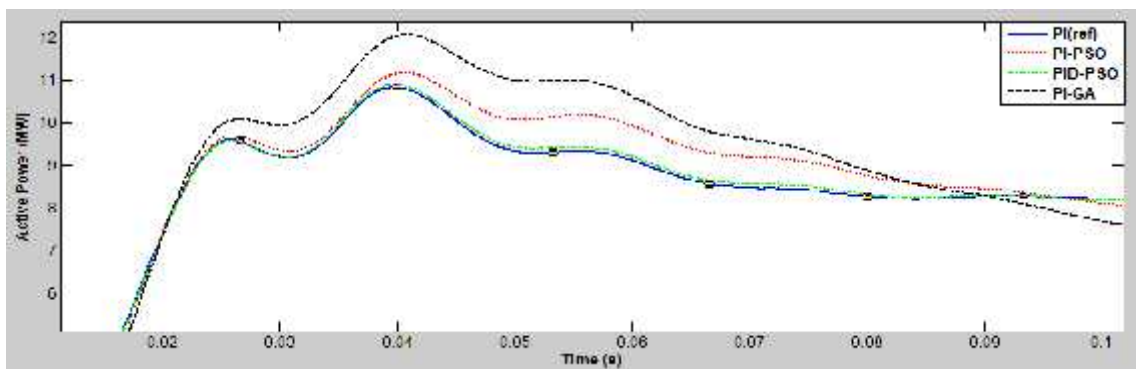


Fig. 8 Active power generated simulation results.

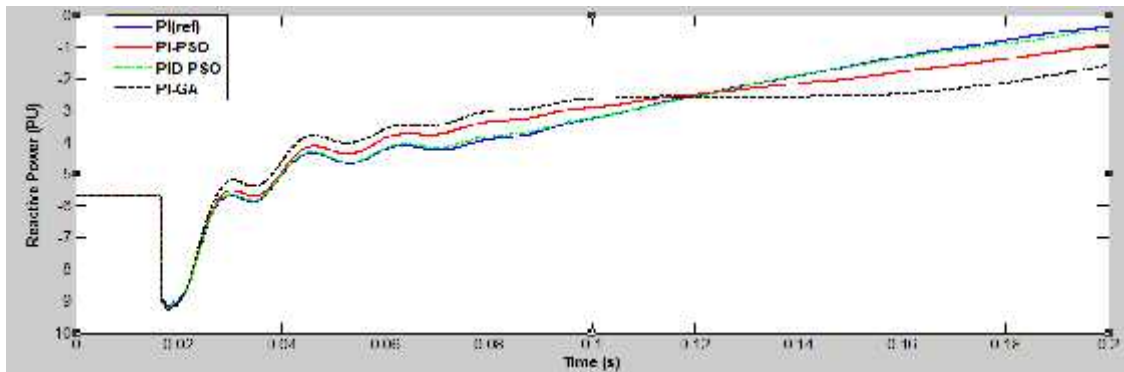


Fig. 9 Active power generated simulation results.

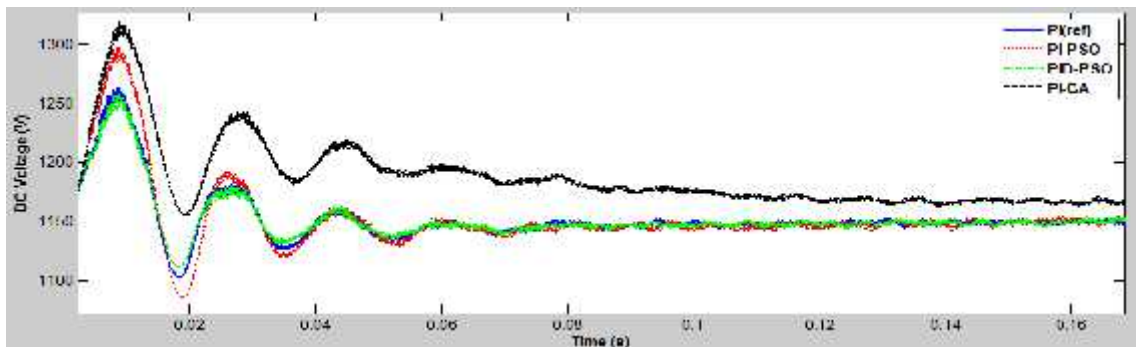


Fig. 10 DC link voltage simulation results.

## VI. SIMULATION RESULTS

In this section, we present the simulation results in MATLAB/SIMULINK to verify the improvement in dynamic response by the optimized PSO-PID controllers of the DFIG based wind farm connected to grid using PSO as shown in Table III.

TABLE III  
 OPTIMAL PARAMETERS FOR CONTROLLERS

Parameter	Pitch angle controller	RSC current regulator	GSC current regulator
$K_p$	3.06	0.5139	0.851
$K_i$	28.1389	8.2049	6.6175
$K_d$	0.032	0.0874	0.0776

Several cases are investigated in our current study as follow:

### A. Case 1: Power System with Large Disturbance

Voltage dip is applied at  $t=0.03$  to 0.3 p.u. of rated grid side voltage. Initially the DFIG wind farm produces 9 MW, the corresponding turbine speed is 1.2 pu of generator synchronous speed, the DC voltage is regulated at 1150 V, and reactive power is kept at 0 Mvar. At  $t=0.03$  s the positive-sequence voltage suddenly drops to 0.5 p.u. causing an oscillation on the DC bus voltage and on the DFIG output power. During the voltage sag the control system tries to regulate DC voltage and reactive power at their set points (1150 V, 0 Mvar). The system recovers in approximately 4 cycles. Active power, reactive power, dc voltage, and the three phase voltage and current curves are shown in Fig. 11 to Fig. 15.

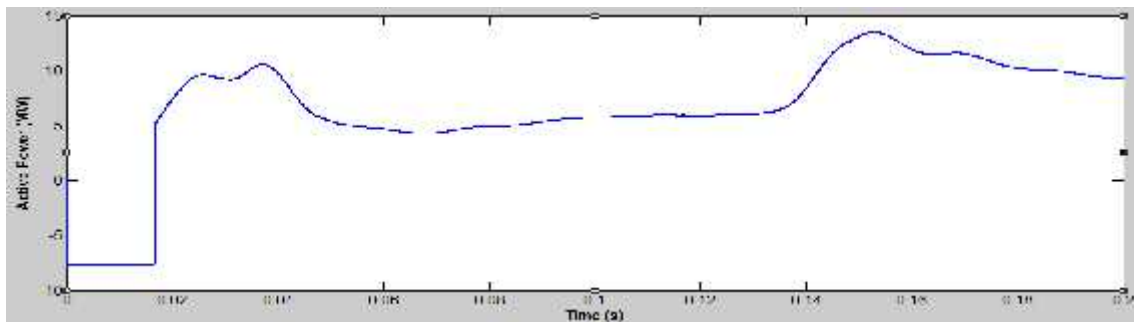


Fig. 11 Active power generated under large disturbance.

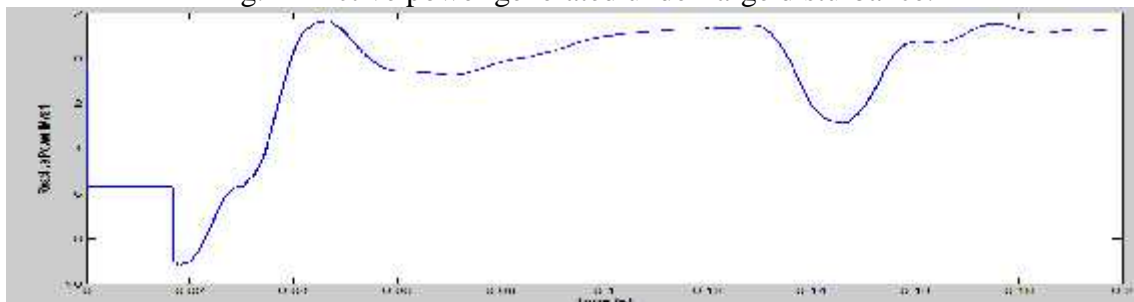


Fig. 12 Reactive power generated under large disturbance.

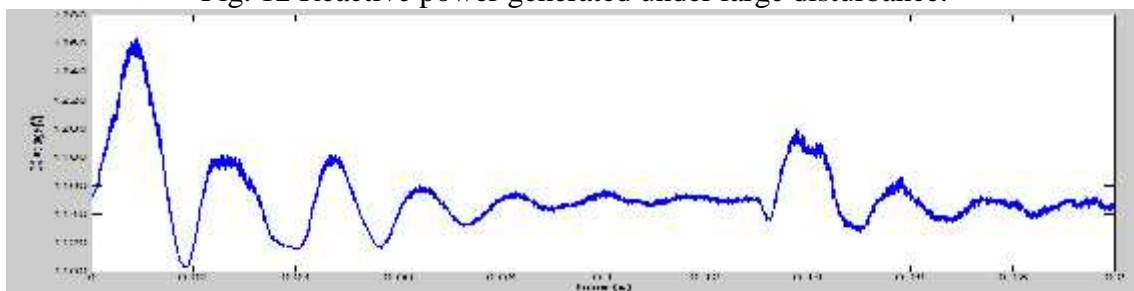


Fig. 13 Dc link voltage under large disturbance.



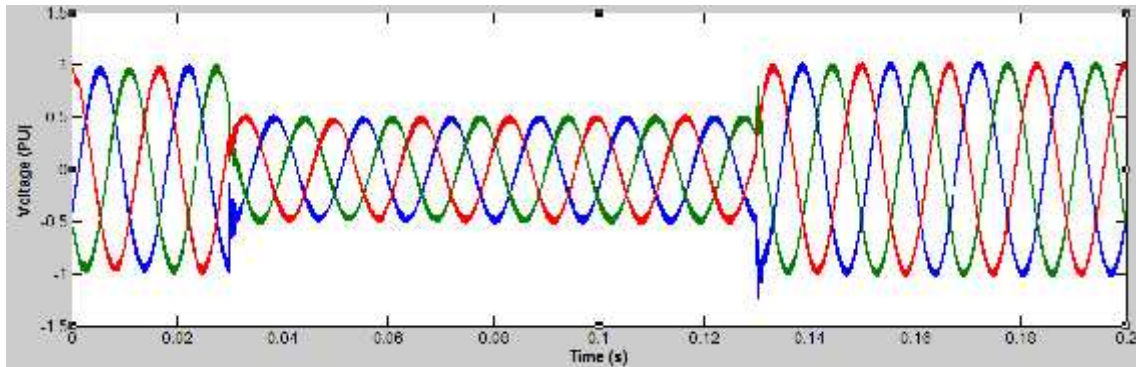


Fig. 14 Three phase voltage at 25kv bus under large disturbance.

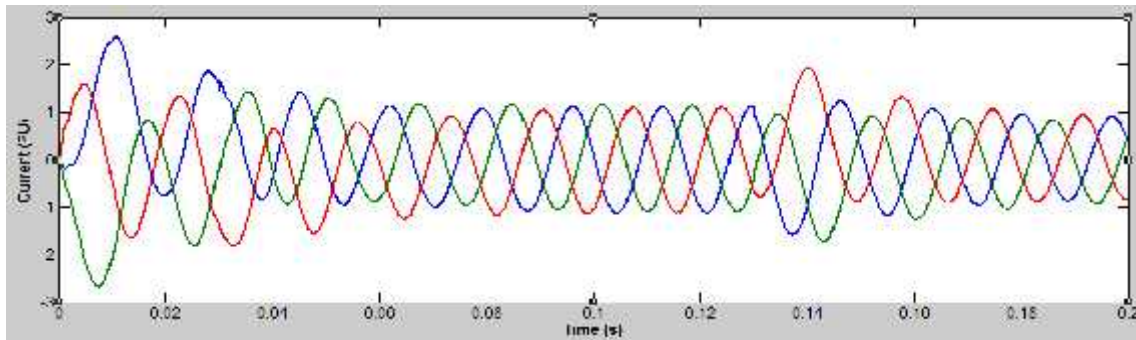


Fig. 15 Three phase current at 25kv bus under large disturbance.

### B. Case 2: Power System with Small Disturbance

Here, a change in wind speed is established. initially, wind speed is set to be at 15 m/s, and then increases to 17 m/s at  $t=0.01s$ . Waveforms for a Gust of Wind illustrates that The generated Active power, reactive power and dc voltage waveforms recovers to their rated values speedily as shown in Fig. 16 to Fig. 18.

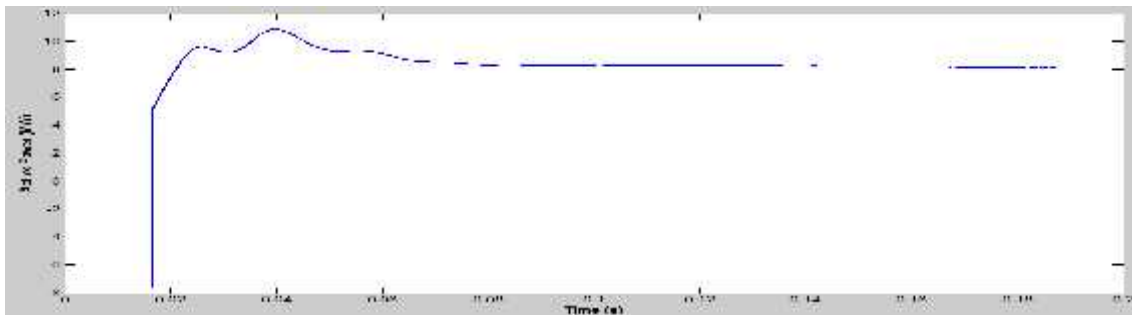


Fig. 16 Active power generated under small disturbance.

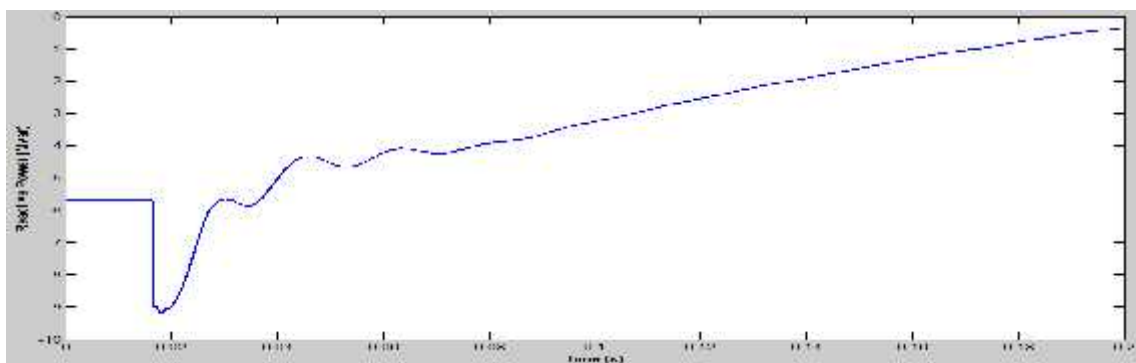


Fig. 17 Reactive power generated under small disturbance.

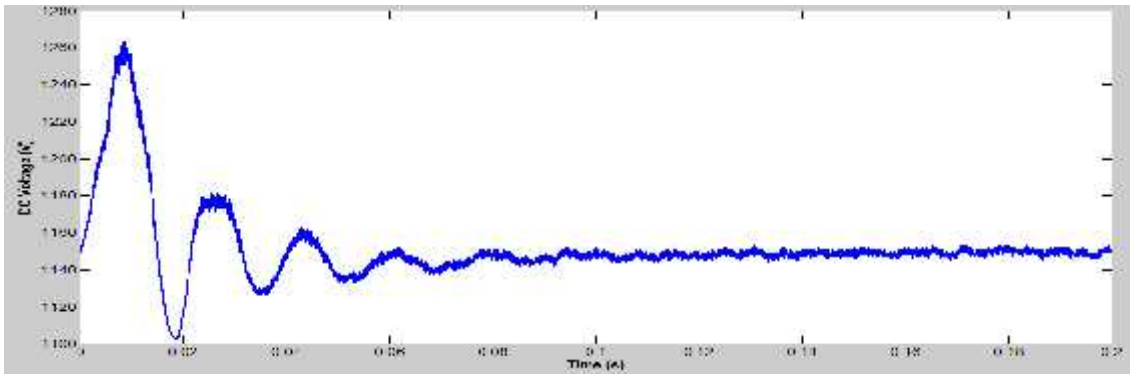


Fig. 18 Dc link voltage under small disturbance.

## VII. CONCLUSION

In this paper, a detailed wind turbine system with DFIG model including induction generator, pitch control, RSC control, and GSC control is presented. A new procedure to tune different types of controllers using PSO aiming to the optimization of desired characteristics response was successfully developed for a DFIG based wind farm connected to grid. The method was validated for both PI and PID controller types and also compared to GA; showing better performance with the additional advantage of simple and robust algorithms for PSO tuned PID controllers.

Simulation results show that the proposed design approach is efficient to find the optimal parameters of the controllers and therefore improves the transient performance of the WTGS over a wide range of operating conditions and different case studies.

## REFERENCES

- [1] A.Grauers, "Efficiency of three wind energy generator system," IEEE Trans.Energy Convers., vol.11,pp. 650–657,1996.
- [2] R. Pena, J. C. Clear, and G. M. Asher, "Doubly fed induction generator using back-to-back PWM converters and its application to variable speed wind energy generation," IEE Proc. Elec. Power Appl., vol. 143, pp. 231–241, 1996.
- [3] F.Wu,X.P.Zhang,K.Godferay,and P.Ju,"Small signal stability analysis and optimal control of a wind turbine with doubly fed induction generator," IETGener.,Transm.,Distrib.,vol.1,pp.751–760,2007.
- [4] L. Yang, G. Y. Yang, Z. Xu, Z. Y. Dong, K. P. Wong, and X. Ma,"Optimal controller design of a doubly-fed induction generator wind turbine system for small signal stability enhancement," IET Gener., Transm., Distrib., vol. 5, pp. 579–597, 2010.
- [5] W. Qiao, J. Liang, G.K. Venayagamoorthy, and R.G. Harley, "Computational intelligence for control of wind turbine generators," in Proc. Power Energy Soc. Gen. Meet., 2011, pp. 1–6.
- [6] H. Huang and C. Y. Chung, "Coordinated damping control design for DFIG-based wind generation considering power output variation," IEEE Trans. Power Syst., vol. 27, no. 4, pp. 1916–1925, 2012.
- [7] P. J. Werbos, "Computational intelligence for the smart grid-history, challenges, and opportunities," IEEE Comput. Intel. Mag.,vol.6,no. 3, pp. 14–21, 2011.
- [8] G. K. Venayagamoorthy, "Dynamic, stochastic, computational, and scalable technologies for smart grids," IEEE Comput.Intel.Mag., vol. 6, no. 3, pp. 22–35, 2011.
- [9] W. Qiao, R. G. Harley, and G.K. Venayagamoorthy, "Coordinated reactive power control of a large wind farm and a STATCOM using heuristic dynamic programming," IEEE Trans. Energy Convers., vol. 24, no. 2, pp. 493–503, 2009.
- [10] Nicholas W. Miller, Juan J. Sanchez-Gasca, and William W. Price Robert W. Delmerico, "Dynamic Modeling OfGe 1.5 And 3.6 Mw Wind Turbine Generators for Stability," IEEE. GE Power systems, GE Research, vol. 6, no. 3, pp. 7803–7989, 2003.